ELSEVIER

Thermochimica Acta 377 (2001) 35–49

thermochimica acta

www.elsevier.com/locate/tca

Adiabatic calorimeter as an ultra-low frequency spectrometer: interplay between phase and glass transitions in solids

H. Suga*

Research Institute for Science and Technology, Kinki University, Higashi-Osaka 577-8502, Japan

Received 30 August 2000; received in revised form 9 January 2001; accepted 15 January 2001

Abstract

Principle and procedure of an adiabatic calorimeter used for an ultra-low frequency spectrometer was described in detail. Structural relaxation in glass-forming liquids and vapor-quenched non-crystalline solids were compared in terms of the Kohlrausch–Williams–Watts' (KWW) empirical equation and the fictive temperature. Kinetic parameters for the structural recovery were analyzed by using the Adam–Gibbs entropy theory. Anomalous behavior of configurational entropy observed for some molecular systems below T_g was discussed. Freezing-in phenomena that occurred in some orientationally disordered crystals (ODC) and anisotropic liquids were described, stressing a wide occurrence of glass transitions in condensed states of matter. Interplay between the phase and glass transitions was discussed in relation to useful dopants which accelerate some molecular motions that had failed to maintain equilibrium at low-temperatures.

Keywords: Relaxation; Glass transition; Configurational entropy; Glassy liquids; Glassy crystals

1. Introduction

Historical development of adiabatic calorimetry traces back to the era of Professor Nernst when he has proposed the heat theorem. Comparison of the calorimetric and spectroscopic entropies in an ideal gas state became the most reliable test of the third law of thermodynamics [1]. Heat capacity data were manipulated to yield the enthalpy, entropy, and Gibbs energy of pure substance [2]. These functions were used to predict the chemical equilibrium constant between any reactants and products. Thus, the low-temperature calorimeter has been one of the central techniques in chemical thermodynamics. The method was continued to use in the materials science developed in 1950s for the clarification of energetic and entropic aspects of new materials.

Phase transitions in crystals have particularly attracted many scientists because of a wide variety of elastic, electric, and magnetic transitions [3,4]. X-ray and neutron diffraction techniques as well as spectroscopic techniques were used in liaison to clarify a microscopic mechanism of the phase transition. The entropy was indispensable quantity in discussing the nature of disorder of system including polymeric materials in relation to the conformational disorder of polymer chain [5]. Thermodynamic characterization of glasses has been done by a low-temperature calorimetry in 1920s [6]. It is impressive to notice that the first observation of glass transition in liquids is more recent than the discovery of radioactivity. Since then,

* Tel.: +81-6-6721-2332; fax: +81-6-6721-2332.
E-mail address: suga@cc.kindai.ac.jp (H. Suga).

0040-6031/01/$ – see front matter
PII: S0040-6031(01)00540-8

various kinds of vitreous solid have been prepared by many methods other than the liquid-quenching [7]. Important keywords for these vitreous solids are the glass transition, residual entropy, structural relaxation, and crystallization. All these processes could be detected by calorimetric measurements [8,9].

It was a natural consequence that the target of calorimetric measurement shifted from the static to dynamic heat capacity. The latter time-dependent property was outside the scope of the calorimetry until Sullivan and Seidel have clearly shown that the heat capacity is a frequency-dependent quantity [10]. Many types of dynamic heat capacity measurements have been proposed since then by using sinusoidal heating [11–13]. Here a brief description is given on an adiabatic calorimeter that can be used as an ultra-low frequency spectrometer for the study of slow dynamics associated with heavily restricted motions in any disordered solids [14]. The real virtue of adiabatic calorimeter as dynamic calorimetry lies in the ability to follow spontaneous temperature change arising from slow enthalpy relaxation in real time extending to 1 Ms.

2. Adiabatic calorimeter as an ultra-low frequency spectrometer

In a low-temperature adiabatic calorimeter, sample either in liquid or solid state is sealed in a vacuum-tight container with a small amount of heat-transmitting medium such as helium gas. There is no special restriction in the size and shape of the calorimetric sample. The calorimetric cell is placed in a highly evacuated and temperature-controlled environment for the realization of adiabatic condition. Under this condition, there is no heat exchange between the calorimetric cell and the surroundings. Thus, all the supplied electrical energy is assumed exactly to be used for raising the sample temperature. The ratio of electrical energy E to the resulting temperature increment ΔT gives the equilibrium heat capacity at average temperature between the initial and final temperatures, $(T_i + T_f)/2$. Attainment of the thermal equilibrium of the sample before and after the energy input is confirmed by the constancy of calorimetric temperature with time during the rating period (the zeroth law of thermodynamics).

Heat can transfer through many routes; convection, conduction and radiation. Owing to this dissipative nature of the heat, realization of the adiabatic condition is not easy. Even with a highly qualified adiabatic calorimeter, a residual heat leakage that induces natural temperature drift amounting to several mK h^{-1} is unavoidable. The drift may be induced by a stray electromotive force generated in differential thermocouples or radiation from surroundings, and is not fluctuating but linear with time. Thus, the temperature versus time curves observed during fore- and after-rating periods are extrapolated to the midpoint of each energizing period to determine T_i and T_f. The process is drawn schematically in Fig. 1 by thick lines which are essentially horizontal in this scale.

A temperature drift whose rate exceeds much that of residual heat leakage appears occasionally, as shown in Fig. 1 by dotted lines. This happens typically around the glass transition temperature T_g of liquids. The spontaneous temperature change arises from irreversible stabilization of liquid structure that has frozen during cooling of the sample. The heat capacity of liquid increases suddenly at T_g over a small temperature interval. Below T_g, the heat capacity is largely due to the vibrations of a disordered solid called glass. Whereas above T_g, the changing structure of the liquid contributes to the heat capacity. This part is called the configurational heat capacity and the corresponding enthalpy is designated as the configurational enthalpy H_c. The relaxation time τ for H_c prolongs drastically at

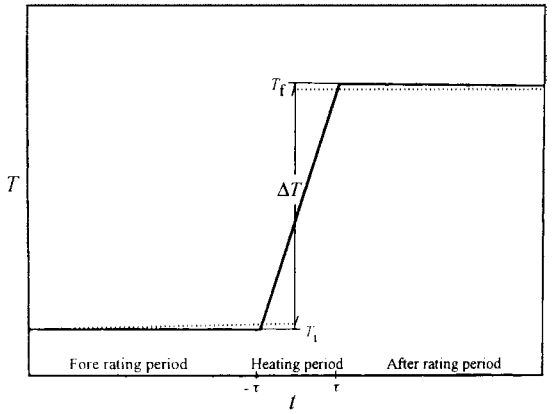

Fig. 1. Principle of heat capacity determination by adiabatic calorimetry. Full line is for equilibrium system, and dotted line for non-equilibrium system.

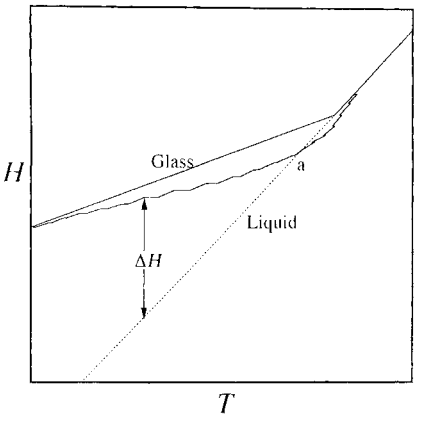

Fig. 2. Schematic drawing of enthalpy (H) vs. temperature (T) curve of substance that undergoes a glass transition T_g on cooling. Zigzag line indicates path that a sample follows during actual heat capacity measurement.

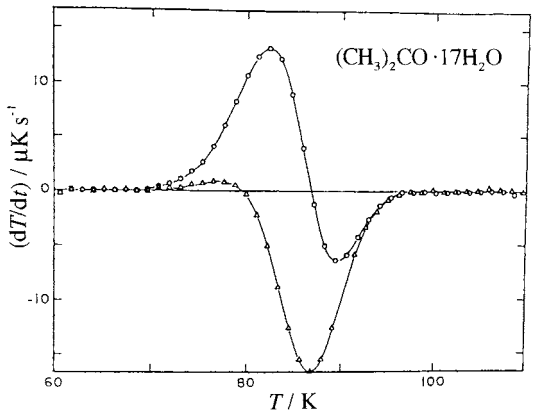

Fig. 3. Spontaneous temperature drift rate observed during equilibration period of acetone hydrate $(CH_3)_2CO{\cdot}17H_2O$ as a function of temperature. Symbol (○) is for a crystal cooled at 0.04 K s^{-1} and symbol (△) for an annealed crystal at 80 K for 30 h after the above experiment.

low-temperatures, whereas that of the vibrational enthalpy H_{vib} is quite short irrespective of temperature.

Fig. 2 draws the enthalpy versus temperature curve of a liquid around T_g observed during heat capacity measurement. An inclined segment shows a temperature increment due to an energy input, and a horizontal segment corresponds to a spontaneous temperature rise or fall due to the enthalpy relaxation. Thus, the observation of a series of exothermic drifts followed by a series of endothermic drifts occurring during the equilibration period is a clear indication that the sample is in a frozen-in disordered state with respect to some degrees of freedom and undergoing structural stabilization towards the equilibrium state. As an example, Fig. 3 shows the rate of spontaneous change in calorimetric temperature observed for acetone (Ac) hydrate $Ac17{\cdot}H_2O$ crystal for two samples. One (symbol ○) was for a crystal cooled at 0.04 K s^{-1} and the other (symbol △) annealed at 80 K for 30 h after the above experiment. The ordinate is average rate observed in the initial 20 min for each equilibration period. At low-temperatures the rate is small because of a long relaxation time even the driving force ΔH is large. Below a certain temperature, the drift rate is too small to follow calorimetrically and the system is in a pseudo-equilibrium state. At high-temperatures, the ΔH value becomes small even the relaxation time is short. There is a temperature at which the rate exhibits a maximum.

The relaxation function of H_c can be described empirically by Kohlrausch–Williams–Watts' (KWW) function [15,16]:

$$\Phi(t) = \frac{\Delta H_c(t)}{\Delta H_c(0)} = \exp\left[\left(-\frac{t}{\tau}\right)^{\beta}\right] \quad (1)$$

where τ is the average relaxation time or the KWW time, and β the non-exponential parameter. It must be recognized that the calorimeter always measures the enthalpy of a sample as a function of temperature. The heat capacity is calculated simply by differentiation of the enthalpy with respect to temperature. Thus, the kinetic parameters governing the enthalpy relaxation can be obtained by analyzing the relaxation function $\Phi(t)$ obtained directly by the calorimetric measurements.

Since the total enthalpy of a sample, $H_{total} = H_{vib} + H_c$, can be kept constant under an adiabatic condition, it follows:

$$\frac{d\Delta H_c}{dt} = -\left[\frac{d\Delta H_{vib}(t)}{dT}\right]\left[\frac{dT}{dt}\right] = -C_{vib}\left[\frac{dT}{dt}\right] \quad (2)$$

Combination of Eqs. (1) and (2) gives the following equation for the calorimetric temperature including any disordered solid as a function of time:

$$T_{vib}(t) = a + bt + c\exp\left[\left(-\frac{t}{\tau}\right)^{\beta}\right] \quad (3)$$

where the second term bt represents the temperature drift rate due to a residual heat leakage. Thus, the

calorimetric temperature observed as a function of time gives independent set of the kinetic parameters. There is no assumption in deriving these kinetic parameters in the present method. The time domain covered by this method is from 0.2 ks to 1 Ms. The upper limit can be extended by prolonged patience of experimentalist and improvement of adiabatic control system.

3. Experimental results

3.1. Heat capacity and residual entropy

Molecular liquids differ from other classes of liquid in being composed of discrete molecules held together by weak intermolecular forces such as isotropic van der Waals and anisotropic hydrogen-bonding forces. Thus, the structure of a molecular liquid tends to change easily with temperature compared to the network liquids. Angell [17] introduced a concept of fragility parameter m in expressing the situation. The idea came from the analysis of the structural relaxation time τ of glass-forming liquid as a function of T. Generally, the logarithm of $\tau(T)$ shows non-Arrhenius behavior. The deviation from Arrhenius behavior is correlated with the parameter m defined as follows:

$$m = \left.\frac{\mathrm{d}\log\tau}{\mathrm{d}(T_{g_\alpha}/T)}\right|_{T=T_{g_\alpha}} \tag{4}$$

Arrhenius behavior is expected when molecular configuration in liquid changes by a process in which some structural units surmount a constant potential barrier. If the barrier height changes with T, non-Arrehnius equation describes the behavior. Phenomenologically, a liquid is classified as fragile when the value m is larger than 17.

Fig. 4 shows the heat capacity (upper) and entropy (lower) of isopropylbenzene [18]. The heat capacity of liquid is much higher than its crystal because the configurational degrees of freedom are easily excited with increased temperature in the liquid but not in the crystal. Thus, the heat capacity of this fragile liquid undergoes a large drop on vitrification at primary T_g or T_{g_α}. On further cooling, the heat capacity exhibits another tiny drop of the heat capacity at secondary T_g or T_{g_β} [19]. This substance is the first example of

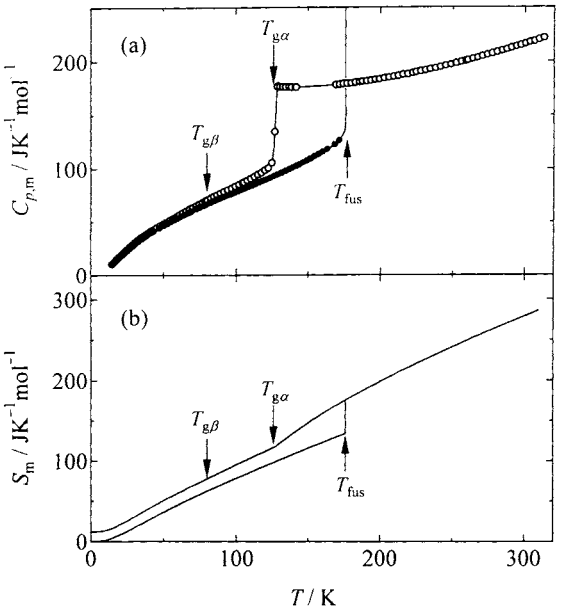

Fig. 4. Heat capacity (a) and entropy (b) of isopropylbenzene. Primary and secondary glass transitions are denoted T_{g_α} and T_{g_β}, respectively.

detecting the T_{g_β} by calorimetric measurement. The drop is quite small but the existence of T_{g_β} is clearly supported by systematic change in the rates of spontaneous temperature drift.

The entropy of liquid exhibits a bend corresponding to the heat capacity drop at T_{g_α} and results in the residual entropy S_0 which measures the frozen-in disorder. In calculating the S_0 value, it is necessary to correct for the entropy production that was produced during the heat capacity measurement due to irreversible structural relaxation. This can be calculated as a problem of a heat conduction between the vibrational reservoir with temperature T and the configurational reservoir with temperature T_{fic}. The concept of fictive temperature T_{fic} was introduced by Tool [20,21] in order to describe the actual frozen structure of any liquids. The T_{fic} for enthalpy can be defined as the temperature at which a glass with a given enthalpy would be at equilibrium if it followed the isoconfigurational enthalpy as the temperature was changed. The amount of irreversible entropy production is quite small for a normally cooled glass, but is not negligible for a vapor-quenched (VQ) glass. This is because the structural relaxation takes place for the VQ glass at

temperatures far below T_g depending on the substrate temperature, as shown later.

The extrapolated entropy of the equilibrated ideal liquid intersects the entropy of the crystal at the Kauzmann temperature T_K [22], at which the configurational entropy of the liquid vanishes. Further extrapolation beyond T_K produces a glass with a negative configurational entropy. In order to save this entropy catastrophe, Gibbs and DiMarzio [23] proposed a thermodynamic second-order phase transition at T_K, and suggested that the actual T_g is a kinetic manifestation of the underlying phase transition. Many other models have been suggested to avoid the entropy crisis since then. Quite recently, Johari [24] proposed that the heat capacity of an equilibrium liquid will decrease along a sigmoid path stretched over a broad temperature range from above T_g to 0 K. He also suggested an experimental resolution for discriminating these models.

3.2. Relaxation in liquids

The enthalpy relaxation process for the structural recovery of glasses can be studied by following the revolution of the glassy structure from a non-equilibrium state into the equilibrium after a step change in temperature or pressure. Relaxation functions for the enthalpy of 1-butene were determined in two ways. One sample was prepared by a rapid-cooling by $-\Delta T_j$ from the equilibrium liquid, and the other by a rapid-heating by ΔT_j from a long-annealed equilibrium liquid. The former sample has an excess configurational enthalpy at the initial stage and exhibits spontaneous exothermic temperature drift under adiabatic condition. The latter has negative initial sign and shows endothermic drift [25]. Both the final temperatures after the relaxation were adjusted to be essentially the same. By integrating the temperature drift rate with respect to time, $\Phi(t)$ of Eq. (1) can be determined experimentally as a function of time.

Fig. 5 represents the reduced enthalpy relaxation function $\Phi_r(t)$ defined as $\Phi_r(t) = -\Delta H_c(t)/|\Delta H_c(0)|$ for both processes. The experiments were carried out at around 58 K. By this definition, $\Phi_r(t)$ changes from 1 to 0 for the positive departure and from -1 to 0 for the negative departure of the initial $H_c(0)$ as the relaxation proceeds. It is clearly shown that the relaxation process is highly asymmetric with respect

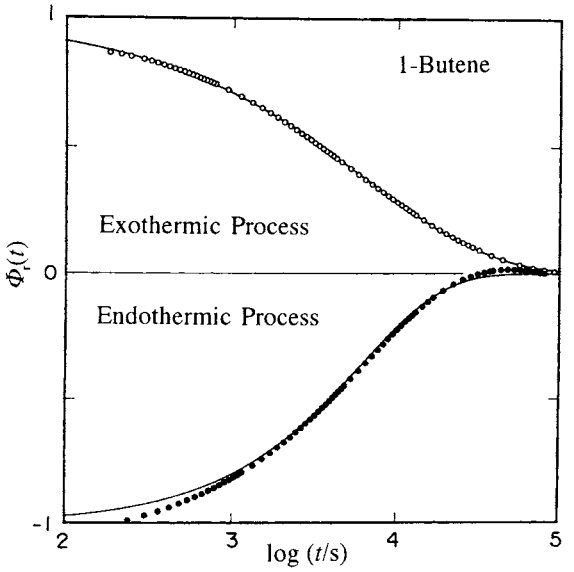

Fig. 5. Reduced enthalpy relaxation function Φ_r of 1-butene plotted as a function of log(t/s). Function $\Phi_r(t)$ is defined as $-\Delta H_c(t)/|\Delta H_c(0)|$ and actual value of $\Delta H_c(0)$ is 115.4 J mol^{-1} for the exothermic and -36.5 J mol^{-1} for the endothermic process, respectively.

to the initial sign of departure. By fitting the data to the KWW Equation (1), following values were derived. For the exothermic process, $\tau = 6.52$ ks and $\beta = 0.56$. For the endothermic process, $\tau = 5.96$ ks and $\beta = 0.84$. The rate of structural recovery differs between the positive and negative values of ΔT_j, depending on whether the relaxation is a structure-breaking or structure-forming process. This indicates non-linear nature of the enthalpy relaxation in molecular liquids, as in the cases of the volume relaxation in some polymer systems [26–28]. Fujimori et al. [29,30] have extended this work by changing the amount of initial departure ΔT_j for glycerol and other glass-forming materials, and found that the parameter β increased linearly with the value ΔT_j. The slope changed a little at $\Delta T_j = 0$, at which the value β_0 will reflect the distribution of relaxation times of the equilibrium liquid. It is noteworthy that the non-linear behavior of the structural recovery can be observed even for very small temperature perturbation. Theoretical approaches to explain and to reproduce these experimental data are highly encouraged.

For a poor glass-forming liquid, vapor condensation technique is powerful in realizing its glassy state.

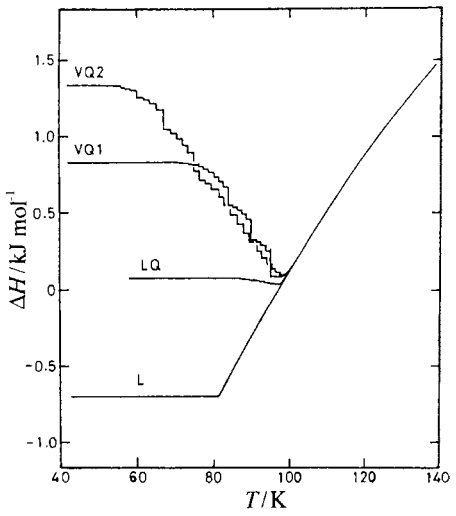

Fig. 6. Configurational enthalpy of butylonitrile prepared by liquid-quenching (LQ) and vapor-quenching (VQ).

A sample vapor is deposited onto a cold substrate under vacuum. During the process the kinetic energy of each molecule is rapidly removed. It is interesting to compare the difference in efficiency by which the molecular energy is extracted between traditional liquid-quenched (LQ) and VQ processes. Fig. 6 gives the configurational enthalpy ΔH_c of butyronitrile glasses [31] produced by LQ and VQ methods. The configurational enthalpy ΔH_c of the equilibrium liquid is denoted as L and that of liquid-quenched sample as LQ. Two kinds of VQ solid were prepared: VQ1 was prepared at a substrate temperature of 67 K and VQ2 at 40 K. These temperatures are far below the value T_K of 81.2 K of this liquid. The reference of ΔH_c was taken to be the value for the LQ sample at the temperature at which the spontaneous temperature drifts changed its sign from positive to negative.

Each curve was calculated using successive backwards integrals of the temperature drift rate with respect to time as well as addition of supplied energy from a fixed temperature of the equilibrium liquid above T_g to the point being determined below T_g. Spontaneous temperature change over a time interval is multiplied by the instantaneous (vibrational) heat capacity to determine the amount of the enthalpy release during that period. The horizontal segment corresponds to the temperature rise due to Joule heating with quasi-isoconfiguration, while the almost vertical segment corresponds to quasi-isothermal enthalpy relaxation towards the equilibrium liquid. The rather long segments in the VQ samples indicate that the spontaneous temperature drifts were followed over a long period. This figure enables us to determine the T_{fic} value of each vitreous state. Thus, the value T_{fic} of VQ2 at the initial state is 134 K, that of VQ1 is 119 K, and that of LQ is 100 K. The results shows that the VQ method produces a vitreous state which deviates from the equilibrium liquid much farther than the LQ solid. The parameter β can be evaluated by transforming the KWW equation in the following way:

$$\log\left\{\log\left[\frac{\Delta H_c(0)}{\Delta H_c(t)}\right]\right\} = \beta \log\left(\frac{t}{s}\right) \tag{5}$$

All the data for the VQ1 sample measured at three temperatures gave good straight lines whose slope is equal to β. The value β was 0.07 at 83.8 K, 0.11 at 89.7 K, and 0.21 at 95.0 K, respectively, and quite different from the values 0.6–0.9 observed for many LQ glasses, indicating a wide distribution of the relaxation times for the VQ solid. Thus, the KWW equation can describe the relaxation behavior of a vitreous solid located far from the equilibrium liquid.

3.3. Configurational entropy

Many models have been proposed to describe the non-Arrhenius behavior of the structural relaxation time τ. Adam and Gibbs [32] derived the following AG equation based on a statistical model:

$$\tau = A \exp\left[\frac{z^* \Delta\mu}{kT}\right] = A \exp\left[\frac{N_A \Delta\mu s_c^*}{kTS_c(T)}\right] \tag{6}$$

where $S_c(T)$ is the macroscopic configurational entropy of liquid, $\Delta\mu$ the chemical potential per molecule hindering the cooperative rearrangement of a group of molecules, z^* the number of molecules constituting the group, s_c^* the configurational entropy of the smallest group that can undergo the rearrangement, and N_A is the Avogadro's constant. The theory asserts that τ depends not only on T but also on $S_c(T)$. The non-Arrhenius behavior may arise from the fact that the number z^* increases with falling temperature and approaches the number of molecules in the system at T_K, at which τ will diverge.

The configurational entropy $S_c(T)$ of a glass with a fictive temperature T_{fic} can be determined by the following equation [33]:

$$S_c = \int_{T_K}^{F_{fic}} \left[\frac{C_c(T)}{T}\right] dT \quad (7)$$

Here, T_K is the Kauzmann temperature and $C_c(T)$ is the configurational heat capacity defined by

$$C_c(T) = C_p^{eq}(T) - C_{vib}^{gl}(T) \quad (8)$$

The first term of the right-hand side denotes the equilibrium heat capacity of liquid and the second term the heat capacity of glass contributed from the vibrational degrees of freedom. Eq. (7) can be rewritten as follows:

$$S_c = S_c(T_{fus}) - \int_{T_{fic}}^{T_{fus}} \left[\frac{C_c(T)}{T}\right] dT \quad (9)$$

For a normally cooled liquid, say with a rate of $-1\ K\ min^{-1}$, the value T_{fic} is nearly equal to T_g. The determination of C_{vib}^{gl} is not easy because lattice dynamical theory has not been well developed for disordered systems. One way to overcome this difficulty is to refer the heat capacity of crystal and to correct for the difference in vibrational entropies between the crystal and glass.

$$S_c(T) = S_c(T_{fus}) - \int_0^{T_{fus}} \left[\frac{C_p^{gl}(T) - C_p^{cr}(T)}{T}\right] dT - \int_T^{T_{fus}} \left[\frac{C_p^{liq}(T) - C_p^{gl}(T)}{T}\right] dT \quad (10)$$

This is the standard formula for the experimental determination of $S_c(T)$ for a glass obtained by a normally cooled liquid. The entropy of fusion is not exactly identical with $S_c(T_{fus})$ because there is a slight difference in vibrational entropies between the glass and crystal. The second term corrects for this effect. A combination of the Debye and Einstein functions is used to reproduce the experimental heat capacities of the crystal and glass at low-temperatures and the best-fit parameters are used to estimate the vibrational entropies at high-temperatures. Fig. 7 represents the enthalpy and entropy of VQ and LQ samples of 1-pentene along with contribution from the vibrational entropy to S_c. The correction for the difference in vibrational entropies is about 5–10% of the entropy difference at T_{fus}.

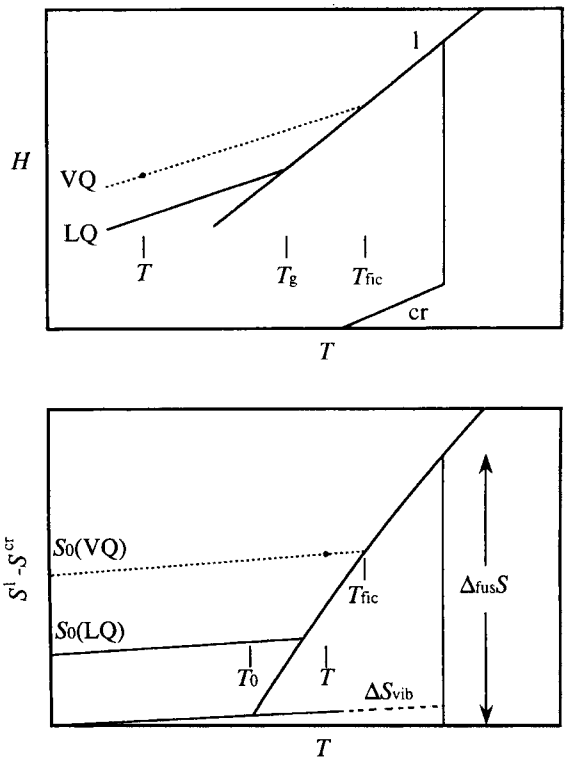

Fig. 7. Enthalpy and entropy of 1-pentene prepared by liquid-quenching (LQ) and vapor-quenching (VQ).

One may notice a long tail of "excess" heat capacity in a glass below T_g (see, for example, in the temperature range 70–130 K in Fig. 4). This long tail always appears in many glass-forming molecular liquids in which the constituent entity has conformational as well as rotational degrees of freedom. There must be some common physical reasons for that. Fig. 8 displays the temperature variations of the configurational entropy S_c for 1-butene ($T_g = 59$ K) [25] and for 1-pentene ($T_g = 68$ K) [33]. The values were calculated based on smooth heat capacity data reproduced by a polynomial function with respect to temperature. The value S_c does not keep constant below T_g as a classical view predicts, but decreases slowly over a wide temperature in a range $0.7 < T/T_g < 1$. This part of the heat capacity is attained rapidly and we must consider about possible sources of this excess heat capacity.It is hard to imagine that the tailing effect

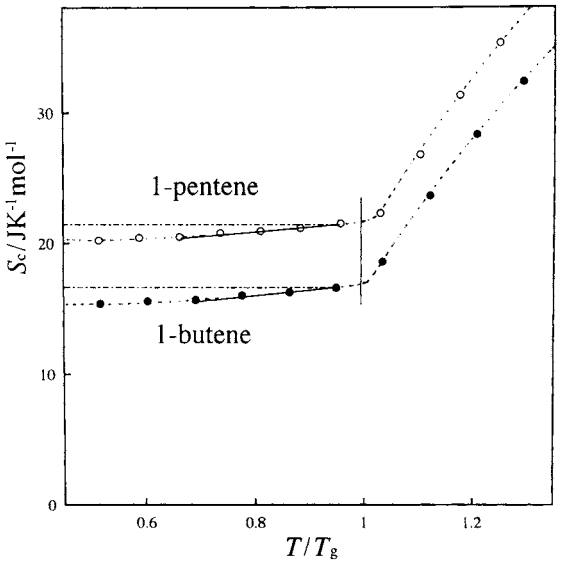

Fig. 8. Configurational entropy S_c of 1-butene and 1-pentene as a function of temperature.

is of vibrational origin, since there is no counterparts in the heat capacity of the crystal. In view of continuity of the tail with the heat capacity jump at T_g, it is considered that the effect is of configurational origin. Molecular glasses have a free-energy landscape possessing a large number of energy valleys separated by energy mountains which arise mainly from the conformational degrees of freedom of the constituting molecules [34]. At high-temperatures the molecules in a fragile liquid are fluctuating among high density of configurational substates. As the temperature is lowered, the fluctuation becomes sluggish and the liquid structure is frozen in a substate. Even in this case, small-scale fluctuation among substates is possible if the barrier heights separating them are less than the molecule thermal energy kT. This thermal excitation can contribute to the heat capacity of the glass below T_g and causes the observed decrease in S_c over a wide range of temperature. The decrease in S_c seems to be proportional to temperature T in some temperature region, as shown by full lines in the figure.

Interestingly, Hutchinson et al. have proposed recently that the configurational entropy S_c for polymers is not constant but decreases with lowering temperature below T_g down to T_K, when the polymer is cooled at a constant rate [35]. This situation is believed to be caused by the distribution of relaxation times in the polymer. They assumed that the configurational entropy S_c can be divided into two terms, one depending on temperature T and the other on fictive temperature T_{fic}.

$$S_c(T, T_{fic}) = x_S S_c(T) + (1 - x_S) S_c(T_{fic}) \tag{11}$$

Here x_S ($0 \leq x_S \leq 1$) is an entropic non-linear parameter analogous to the parameter x involved in the Tool [20,21]–Narayanaswamy [36]–Moynihan [37] (TNM) equation for the structural relaxation time $\tau(T, T_{fic})$.

$$\tau(T, T_{fic}) = \tau_0 \exp\left[\frac{x\,\Delta h^*}{RT} + \frac{(1-x)\Delta h^*}{RT_{fic}}\right] \tag{12}$$

We should analyze many heat capacity data of the glass-forming molecular liquids to confirm their general occurrence of the heat-capacity tailing effect.

For the AG equation to be tested experimentally, it is necessary to determine the value of $S_c(T)$ at each moment of the structural relaxation to be correlated with τ under non-equilibrium condition [31]. This quantity $S_c(T)$ cannot be measured directly by calorimetry, but can be determined through the fictive temperature T_{fic}. Fig. 9 illustrates the actual procedure for the determination of $S_c(T)$ of butyronitrile sample

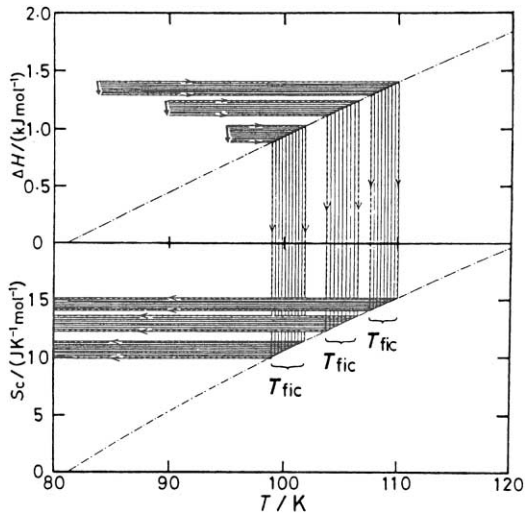

Fig. 9. Determination of configurational entropy S_c for butyronitrile at each moment during a structural relaxation experiment through fictive temperature T_{fic}. Three stripes correspond to three experiments carried out at 83.8, 89.7, and 95.0 K, respectively.

at each moment of the relaxation. Three stripes correspond to three experiments for the structural relaxations taken at three different temperatures, 83.8, 89.7, and 95.0 K, respectively. The upper and lower dot-and-dash curves show the H_c and S_c of an equilibrium liquid plotted against T. Both values can be calculated by the experimental heat capacity of the equilibrium liquid and the extrapolated values down to lower temperatures. Solid arrows in the upper portion show the enthalpy relaxation observed in the actual experiment. From the plot, the value T_{fic} can be determined, and the value is used to determine the experimentally inaccessible value S_c at that moment. The AG equation can be rearranged into the following form:

$$\log \tau = \log A + \left(\frac{\Delta \mu s_c^*}{TS_c} \right) \tag{13}$$

Fig. 10 shows plots of log τ versus $(TS_c)^{-1}$ at the three temperatures. There is no fitting parameter in this procedure. All the curves give nearly straight lines, implying that $\Delta \mu s_c^*$ is almost constant during the relaxation at each temperature. Increasing temperature causes the slope and, hence, $\Delta \mu s_c^*$ to decrease. The structural relaxation that took place at temperatures far below T_K for the VQ samples is due to its high S_c values. Similar results were obtained for VQ and LQ solids of 1-pentene [33]. In this way, the AG equation seems to be valid for the description of the relaxation times of glasses that are located far from the equilibrium state.

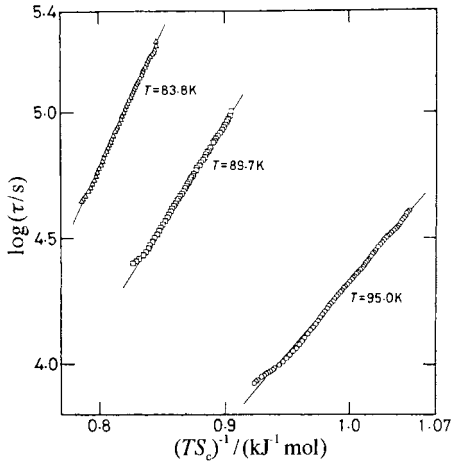

Fig. 10. Plot of log τ against $(TS_c)^{-1}$ for a vapor-quenched sample of butyronitrile.

Another test for the validity of the AG theory can be done by using densified glasses. The value T_g is operationally defined as the temperature at which the relaxation time becomes a time-scale for a single heat capacity determination, say 1 ks. The AG theory requires that the glass transition should take place at a temperature at which TS_c becomes constant for glasses produced at various pressures for one substance. On the other hand, iso-S_c state for T_g was proposed by Bestul and Chang [38]. For the experimental test, a high-pressure adiabatic calorimeter workable up to 0.3 GPa using He gas as a pressure-transmitting medium was developed [39]. The essential feature of this calorimeter is to keep a pre-determined pressure over the entire temperature range using a negative feedback system. Any pressure change in the calorimetric system is detected by a Manganin wire held in a thermostatted bath. The wire constitutes one arm of a Wheatstone bridge and the output signal is used to control the temperature of He gas in a pressure reservoir after amplification. The pressure variation inside the calorimetric cell can be kept within ±0.1 MPa over the temperature range between 30 and 350 K.

The heat capacities of 1-propanol and 3-methylpentane for their crystalline and liquid states were measured at three pressures, respectively [40]. The observed T_g value was 96.2 K at 0.1 MPa, 103.8 K at 108.4 MPa, 109.1 K at 198.6 MPa for the former, and 77.0 K at 0.1 MPa, 85.3 K at 108.1 MPa, 91.8 K at 198.5 MPa for the latter. Experimental data for the entropy of fusion and heat capacity difference between the crystal and liquid were combined to calculate the temperature dependence of the configurational entropy S_c at each pressure. The results are summarized in Fig. 11 for the two compounds. It is concluded that the quantity TS_c becomes constant at T_g irrespective of the applied initial pressure within experimental uncertainty for both compounds, indicating the validity of the AG entropy theory.

3.4. Prigogine–Defay ratio

For a non-equilibrium system, it is not possible to describe any states of the system only by two external parameters such as T and p. It has been proposed that the thermodynamic properties of liquids near T_g may be specified by a set of order parameters $\{z\}$, the

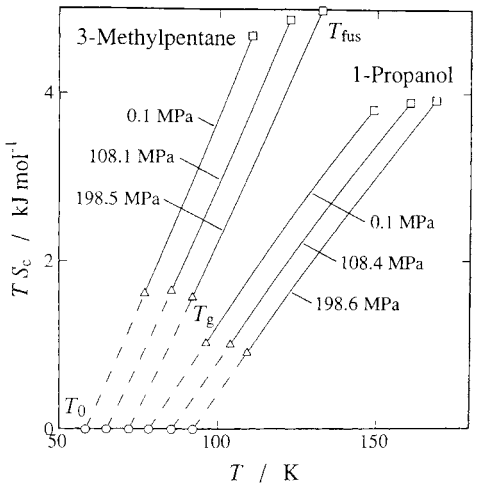

Fig. 11. Plot of $(TS_c)^{-1}$ at T_g of 3-methylpentane and 1-propanol under various applied pressures.

values being functions of T and p at equilibrium, but remaining constant in the glass at the values they have at T_g. Experimental data may be used to clarify about the question "how many order parameters are required for the thermodynamic description of glass?" Davies and Jones [41] have discussed first this problem and proposed to test the inequality $\Delta\kappa/\Delta\alpha \geq TV\Delta\alpha/\Delta C_p$, where $\Delta\alpha$ is the jump of thermal expansivity, $\Delta\kappa$ the jump of isothermal compressibility, and ΔC_p is the jump of heat capacity at T_g, respectively. If they are equal, single parameter is sufficient. If inequality holds, two or more parameters are necessary. Some experimental data indicate that the $\Delta\kappa/\Delta\alpha$ is almost twice $TV\,\Delta\alpha/\Delta C_p$, and hence, a single order parameter is not sufficient. Nowadays, the following quantity is designated as the Prigogine–Defay ratio Π [42].

$$\Pi = \frac{\Delta C_p \Delta\kappa}{TV(\Delta\alpha)^2} \tag{14}$$

The equation reminds us the Ehrenfest relation for the second-order phase transition. Gupta and Moynihan [43] have derived the relation $\Pi \geq 1$ for systems whose states need to be specified in terms of a number of $\{z\}$ by considering the conditions of tangency of the Gibbs energy surfaces of an equilibrium liquid and of a glass with constant values of $\{z\}$. The relevance of the quantity Π to the kinetics of the structural relaxation in glass was discussed based on the calculation. It was concluded that different relaxation kinetics should be observed for the approach of the volume V and enthalpy H of glasses to equilibrium for any systems with $\Pi > 1$.

There have been hot discussions about the experimental determination of Π. The main point is that a combination of thermodynamic values from various literature sources is not appropriate. Any non-equilibrium state cannot be reproduced in different experiments with different thermodynamic paths and different experimental time scales. Different batch of the same substance cannot guarantee the same relaxation behavior, because small amounts of impurities seriously affect sometimes the relaxation kinetics.

In order to resolve these experimental problems, we have developed a novel adiabatic calorimeter for simultaneous measurement of the H and V [44]. The calorimeter works under constant pressure up to 100 MPa in the temperature range 80–380 K. Sample is pressurized hydrostatically by using a liquid pressure-transmitting medium. The sample volume is measured with a new type of highly-sensitive dilatometer using bellows which expands or contracts smoothly so as to balance the pressure of sample with the applied pressure. The location of the bellows is determined by a magnetic system with a precision of ± 0.1 μm. This allows to determine the volume change to ± 0.1 ppm of the sample volume.

Takahara et al. [45] used this calorimeter to determine the values $\Delta\kappa$, $\Delta\alpha$, and ΔC_p of atactic polystyrene ($T_g = 353 \pm 0.3$ K) and of a molecular mixture $[(o\text{-terphenyl})_{0.67} + (o\text{-phenylphenol})_{0.33}]$ ($T_g = 253.7 \pm 0.2$ K). Careful analyses of the experimental data gave $\Pi = 1.3 \pm 0.1$ for the former, and $\Pi = 1.2 \pm 0.05$ for the latter, respectively. They also used the apparatus to determine the relaxation rates for the enthalpy and volume of both substances using a pressure- and temperature-jump methods. They found that the volume relaxed faster than the enthalpy and the relaxation paths for the V and H did not coincide with the equilibrium lines. The conclusion is that one parameter is not sufficient to describe thermodynamically the glassy states of both substances. Gupta has proposed a concept of fictive pressure p_{fic} in addition to T_{fic} [46]. It is highly desired to collect such beautiful experimental data for many systems.

3.5. Glass transition in mesophase

Crystals and glasses are the two extremes in our concepts of structural regularity in solids. There exist various kinds of solids which have intermediate nature of disorder. The one is a group of glassy states of anisotropic liquid or liquid crystals (LC). The other is a group of glassy states of isotropic crystals or orientationally disordered crystals (ODC). Particularly the latter crystals are intriguing solids, because crystals and glasses are contradicting each other in their concept. Most of the molecular crystals fuse directly into isotropic liquids. Some crystals fuse in two steps, either through the LC phases or ODC phases. If these phases are cooled rapidly for by-passing the transformation into ordered crystals, the undercooled phases undergo freezing-in process at a temperature at which the relevant relaxation time τ crosses the experimental time, as in the case of ordinary glasses [47–50].

Analogy between the dielectric and enthalpy relaxation will be helpful in understanding the concept of glassy crystals. Dipolar liquids generally exhibit the dielectric relaxation in the equilibrium or undercooled liquid phases depending on the frequency f of external electric field. The dielectric permittivity drops at a temperature at which the dielectric relaxation time τ_d becomes $(2\pi f)^{-1}$, indicating a freezing-in of the orientation polarization. The actual T_g value of the liquid corresponds to the temperature at which the value τ_d becomes $\sim$1 ks. The same thing can happen in some ODC in which the centres-of-mass of the molecules form three-dimensional periodical lattice but their orientations are random among several equi-energetical directions, say [1 1 1] directions of their fcc or bcc lattices. The reorientational motion is dynamic at high-temperatures but becomes quiet as the temperature is lowered until the motion becomes dormant. The heat capacity drops suddenly more or less in a narrow temperature range just in a way similar to the liquids. Obviously the orientationally glassy state should be extended to crystals which are composed of non-polar molecules. In spite of the paradoxical nature of the concepts involved in the terminology, time is now giving it proof as an intriguing new state of aggregation of molecules [51,52].

Fig. 12 displays the heat capacity (upper) and entropy (lower) of cyclohexanol, which forms an fcc lattice below T_{fus}. The high crystallographic

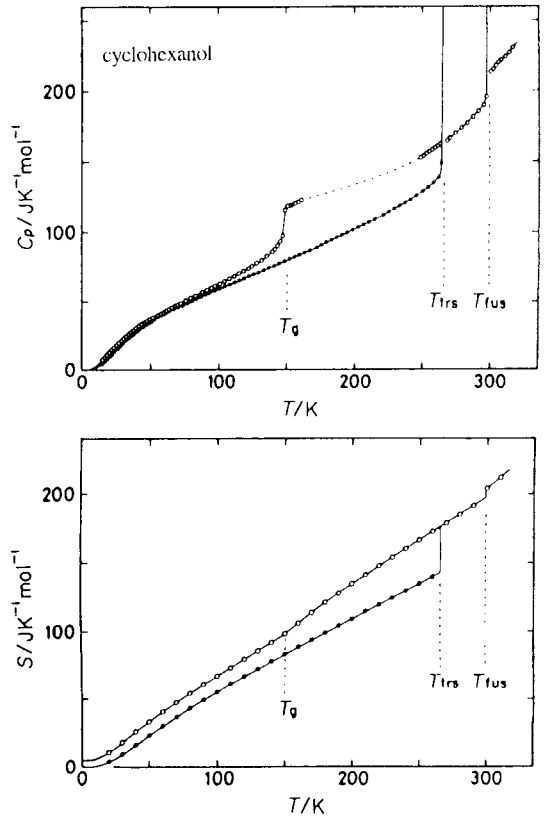

Fig. 12. Heat capacity (upper) and entropy (lower) of cyclohexanol. Symbol (●) is for stable crystalline phase and symbol (○) is for undercooled high-temperature phase.

symmetry arises entirely from a great deal of orientational disorder of the molecules that have only a mirror symmetry at the best. When the ODC phase is cooled by avoiding the transformation into an ordered low-temperature phase, the undercooled ODC phase exhibits T_{g_α} at about 150 K [53–55]. The entropy curve shows a bend at the temperature and the remaining disorder reveals itself as the residual entropy. Again the heat-capacity tail below T_g is noticeable. In this case, both the reorientational motion of molecules as well as the conformational motion between the axial and equatorial forms are frozen-in below T_g. The long heat-capacity tail below T_g causes the S_c to decrease over a wide range of temperature, as in the cases of glassy liquids already mentioned.

The undercooled ODC phase shows a relaxation map similar to those of liquids, as shown in Fig. 13.

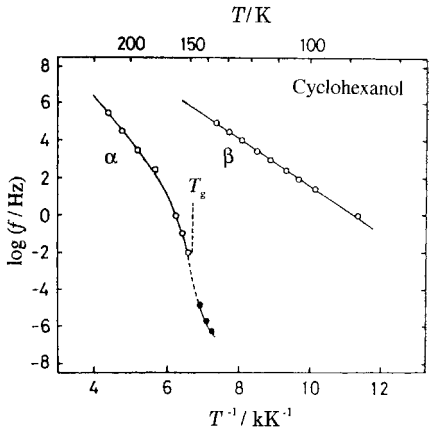

Fig. 13. Relaxation map of cyclohexanol crystal determined dielectrically (○) and calorimetrically (●).

The corresponding T_{g_β} appears at about 65 K. The behavior is unable to discriminate in all aspects from ordinary glasses only except for the existence of a long-range positional order. In the case of ethanol, two kinds of T_{g_α} were observed for its liquid and ODC phases, respectively. This observation suggests that reorientational motion of molecules commonly taking place in both phases will govern the kinetics of the relaxation process. In the case of isocyanocyclohexane crystal, a tiny T_g appeared above T_{g_α} [56]. The process turned out to be due to freezing-in of the axial-equatorial conformational change of molecules located on an fcc lattice. These many observations clearly indicate that the glass transitions are not characteristic of liquids but of wide occurrence in condensed matters in relation to freezing out of some molecular motions due to prolonged relaxation time.

The situation is not limited to the metastable undercooled phase of crystal. Observation of residual entropy in ice crystal I_h is the most familiar example of freezing-out of molecular motions in the stable crystalline phase. The half-hydrogen model proposed by Pauling cannot be an equilibrium structure of ice that satisfies the third law of thermodynamics, but absence of any anomalous heat capacity that can be ascribed to an ordering transition has puzzled many scientists for a long time [57]. The dielectric and enthalpy relaxation times of ice, τ_d and τ, turned out to lie on the same straight line in an Arrhenius plot [58]. Extrapolation of these data to 60 K, a hypothetical ordering temperature proposed by Pitzer and Polissar, gave a value τ of 10^{13} s. It must be this geological time which hindered the crystal from realizing an ordered structure of hexagonal ice in our laboratory time.

A minute amount of alkali hydroxide doped into the ice lattice was found to accelerate dramatically the reorientational motion of water dipoles [59–61]. Thus, an ice sample doped with KOH in the mole fraction of 2×10^{-5} induced a first-order phase transition at 72 K, which removed a substantial fraction of the residual entropy and changed the lattice symmetry from $P6_3/mmc$ to $Cmc2_1$. Our experiments are always controlled by Deborah number *De* [62] defined as the ratio of the relaxation time and observation time. As far as $De \ll 1$, we can observe the whole shape of heat capacity anomaly associated with the possible ordering transition that can be determined by intermolecular interaction and cooperative nature of the interaction. For a system $De \gg 1$, we will miss a part or full of the anomalous thermodynamic quantity owing to our limited experimental time. The relaxation time is governed by disordered structure and barrier height hindering the rearrangement of the structure. Whether the disorder should be described as static or dynamic depends inter alia on the height of potential barrier, temperature and time-scale of the experiment. A particular impurity doped into the system will modify the cooperative nature of the rearrangement and reduce the relaxation time as a whole. Only this process makes possible to observe a transition which has been concealed for a kinetic reason. Modification of chemical potential of a system by that of a particular impurity can result in a drastic change of dynamical situation of the system. We may call this new field the ''doping chemistry''.

A similar disorder of water molecules can be found in clathrate hydrates. The host lattice of the crystals forms various types of Archimedean polyhedral cages composed of hydrogen-bonded water molecules, and accommodates a variety of guest molecules of suitable size. For the hydrates enclathrating dipolar guest molecules, two dielectric relaxation are known; the one is associated with water dipoles and the other the guest dipoles. Dynamic behavior of the host and guest molecules has been extensively studied [63], but no successful observation of any ordering transition has been another puzzling problem in this field. Thus, the

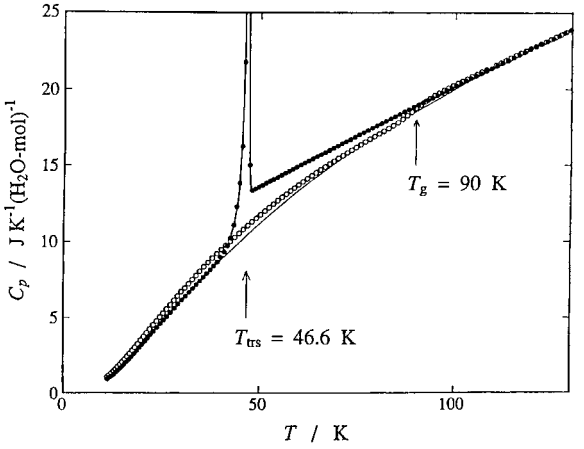

Fig. 14. Heat capacity of pure (○) and KOH-doped (●) acetone clathrate hydrate crystal $(CH_3)_2CO{\cdot}17H_2O$.

dopant experiment was tried again to this binary system to find out an expected ordering transition.

Fig. 14 shows the heat capacities of pure and KOH-doped (10^{-5} mole fraction) Ac·17H$_2$O hydrate crystals [64,65]. The pure crystal (open circle) exhibited a tiny heat capacity anomaly at around 90 K, and the effect may be overlooked without intentional examination. However, the associated spontaneous temperature drifts (see Fig. 3) is a clear indication of the freezing process taking place in the crystal. The first-order phase transition was induced at 46.6 K by a catalytic action of the small amount of KOH dopant. Dielectric measurement showed that both the host and guest molecules were ordered in the low-temperature phase. Most probably, the ordering of the host water dipoles produced a strong electric field which forced the guest molecules to align along a preferred orientation. Phase transition was also induced by this way in the clathrate hydrate enclathrating tetrahydrofuran, trimethylene oxide, and others. A particular kind of dopant acted on frozen-in disordered system as catalyst for releasing the immobilized state and recovering the equilibrium state in our observation time. The relaxation time data of pure and doped ices and some clathrate hydrates are drawn in Fig. 15 as a function of temperature [64,65]. The dielectric relaxation time of pure and doped ices were measured by Kawada [66,67]. It is noteworthy that the dopant KOH not only shortens the relaxation time but also reduces largely the activation energy. The latter effect is particularly important for observing the ordering transition that occurs at low-temperatures. In relation to this fact, one might raise an inquiry "what kind of physical or chemical impurity will release the frozen-in state of the liquid?". If a particular dopant be discovered luckily for this purpose, we will be blessed to observe in reality what will happen at the Kauzmann temperature. As a matter of fact, it is not

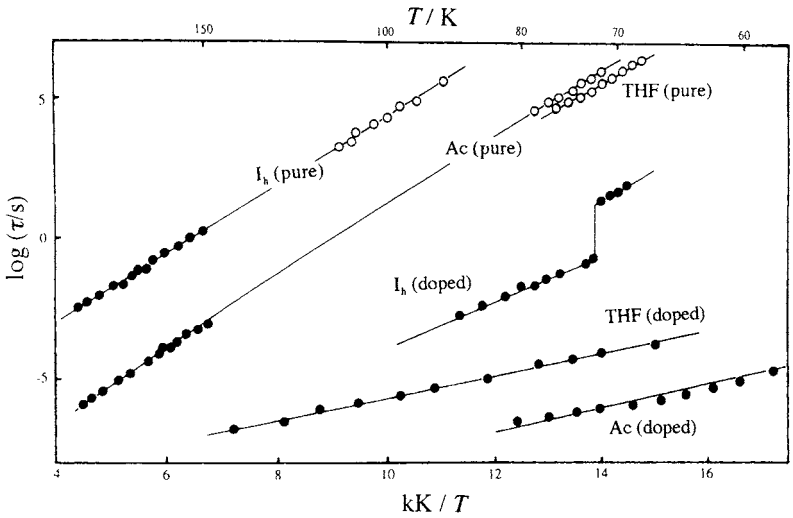

Fig. 15. Relaxation time vs. reciprocal temperature for pure and KOH-doped ices and some clathrate hydrates. I$_h$: hexagonal ice; Ac hydrate: acetone·17H$_2$O; THF hydrate: tetrahydrofuran·17H$_2$O.

easy for us to imagine some disordered solids without any configurational entropy.

There has been significant progress in the theoretical approach by the mode-coupling theory of the glass transition during the last decade. The theory predicts existence of critical behavior around T_c at which decoupling between different relaxation processes, a and b, takes place [68]. At the moment, there is no clear evidence that supports the suggested critical behavior [69]. A new proposal of second critical point between two distinct glassy forms, i.e. low- and high-density amorphous ice, is more realistic based on firm experimental observations. The review article [70] on this topics describes well the situation why the glass transition is still charming and important problem to be challenged.

4. Conclusions

From the servey of the experimental works on glassy states of matters that have been done and are still carried out at Osaka University, the following main conclusions can be drawn.

1. Adiabatic calorimeter can be operated as an ultra-low frequency spectrometer in addition to the traditional role of determination of the heat capacity. The better the quality of the adiabatic control, the clearer the anomalous effects associated with any relaxation behavior. The time domain covered by this method is 0.1 ks–1 Ms and is complementary with the dielectric spectroscopy.
2. Non-crystalline solids can be produced in many ways other than the conventional liquid-cooling. All the non-crystalline solids exhibit commonly glass transition, residual entropy, structural relaxation, and crystallization. The amount of excess enthalpy and the rate of structural relaxation depend strongly on the manner by which the non-crystalline solid was prepared. The relaxation rate can be related with the configurational entropy S_c and temperature T.
3. The glass transitions are not characteristic property of liquids but of wide occurrence in condensed matters in relation to freezing of some degrees of freedom involved in any disordered systems. Thus, glassy LC, glassy crystals were discovered in addition to ordinary glassy liquids. In some cases, multiple glass transitions were observed in one and the same substance.
4. Apparent deviation of some kinds of crystal from the third law of thermodynamics derives from extremely sluggish nature of ordering process compared to the laboratory time. A minute amount of particular kind of dopant happens to accelerate dramatically the process in several crystals to recover their equilibrium states (doping chemistry).

Acknowledgements

Most of the works presented here were done at Osaka University when the author was in active services. The author would like to express his sincere thanks to late Professor I. Nitta and Professor S. Seki who introduced him to this field. The works have been actively continued by many enthusiastic collaborators, to whom the author's thanks are due. Useful discussions with Professor M. Oguni (now Tokyo Institute of Technology), Dr. K. Takeda (now Naruto University of Education), Professor T. Matsuo and Dr. O. Yamamuro are particularly acknowledged.

References

[1] J. Wilks, The Third Law of Thermodynamics, Oxford University Press, Oxford, 1961.
[2] J.P. McCullough, D.W. Scott (Eds.), Experimental Thermodynamics: Calorimetry of Non-reacting Systems, Vol. I, IUPAC, Butterworths, London, 1968.
[3] N.G. Parsonage, L.A.K. Staveley, Disorder in Crystals, Clarendon Press, Oxford, 1978.
[4] H.E. Stanley, Introduction to Phase Transition and Critical Phenomena, Clarendon Press, Oxford, 1981.
[5] P.J. Flory, Principles of Polymer Chemistry, Cornell University Press, Ithaca, 1964.
[6] F.E. Simon, F. Lange, Z. Phys. 38 (1926) 370.
[7] J.D. Mackenzie (Ed.), Modern Aspects of the Vitreous State, Butterworths, London, 1964.
[8] H. Suga, S. Seki, J. Non-Cryst. Solids 16 (1974) 171.
[9] H. Suga, S. Seki, Faraday Discuss. 69 (1980) 447.
[10] P.F. Sullivan, G. Seidel, Phys. Rev. 173 (1968) 679.
[11] I. Hatta, A.J. Ikushima, J. Appl. Phys. Jpn. 20 (1981) 1995.
[12] N.O. Birge, S.R. Nagel, Phys. Rev. Lett. 54 (1985) 2674.
[13] P.S. Gill, S.R. Sauerbrunn, M. Reading, J. Thermodyn. Anal. 40 (1995) 931.

[14] H. Suga, T. Matsuo, Pure Appl. Chem. 61 (1989) 1123.
[15] R. Kohlrausch, Ann. Phys. Leipzig 12 (1847) 393.
[16] G. Williams, D.C. Watts, Trans. Faraday Soc. 66 (1970) 80.
[17] C.A. Angell, J. Non-Cryst. Solids 13 (1991) 131.
[18] K. Kishimoto, H. Suga, S. Seki, Bull. Chem. Soc. Jpn. 46 (1973) 3020.
[19] G.P. Johari, M. Goldstein, J. Chem. Phys. 53 (1970) 2372.
[20] A.Q. Tool, J. Am. Ceram. Soc. 29 (1946) 240.
[21] A.Q. Tool, J. Am. Ceram. Soc. 31 (1948) 177.
[22] W. Kauzmann, Chem. Rev. 43 (1948) 219.
[23] J.H. Gibbs, E.A. DiMarzio, J. Chem. Phys. 28 (1958) 373, 807.
[24] G.P. Johari, J. Chem. Phys. 113 (2000) 1.
[25] K. Takeda, O. Yamamuro, H. Suga, J. Phys. Chem. Solids 52 (1991) 607.
[26] K. Kovacs, Fortschr. Hochpolym-Forsch. 3 (1964) 394.
[27] K. Kovacs, Fortschr, Ann. N.Y. Acad. Sci. 371 (1981) 38.
[28] R.W. Rendell, K.L. Ngai, G.R. Fonk, J.J. Aklonis, Macromolecules 20 (1987) 1070.
[29] H. Fujimori, Y. Adachi, M. Oguni, Phys. Rev. B 46 (1992) 14501.
[30] H. Fujimori, M. Oguni, J. Non-Cryst. Solids 172–174 (1994) 601.
[31] M. Oguni, H. Hikawa, H. Suga, Thermochim. Acta 158 (1990) 143.
[32] G. Adam, J.H. Gibbs, J. Chem. Phys. 43 (1965) 139.
[33] K.Takeda.O. Yamamuro, H. Suga, J. Phys. Chem. 99 (1995) 62.
[34] C.A. Angell, J. Phys. Chem. Solids 49 (1988) 863.
[35] J.M. Hutchinson, S. Montserrat, Y. Calventus, P. Cortes, Macromolecules 33 (2000) 5252.
[36] O.S. Narayanaswamy, J. Am. Ceram. Soc. 54 (1971) 491.
[37] C.T. Moynihan, J.A. Easteal, M.A. DeBolt, J. Tucker, J. Am. Ceram. Soc. 59 (1976) 12.
[38] A.B. Bestul, S.S. Chang, J. Chem. Phys. 40 (1964) 3731.
[39] O. Yamamuro, M. Oguni, T. Matsuo, H. Suga, Bull. Chem. Soc. Jpn. 60 (1987) 1269.
[40] S. Takahara, O. Yamamuro, H. Suga, J. Non-Cryst. Solids 171 (1994) 259.
[41] R.O. Davies, G.O. Jones, Adv. Phys. 2 (1953) 370.
[42] I. Prigogine, R. Defay, Chemical Thermodynamics, Longmans Green, New York, 1954.
[43] P.K. Gupta, C.T. Moynihan, J. Chem. Phys. 65 (1976) 4136.
[44] S. Takahara, O. Yamamuro, M. Ishikawa, T. Matsuo, H. Suga, Rev. Sci. Instrum. 69 (1998) 185.
[45] S. Takahara, M. Ishikawa, O. Yamamuro, T. Matsuo, J. Phys. Chem. 103 (1999) 792.
[46] P.K. Gupta, J. Non-Cryst. Solids 102 (1988) 231.
[47] H. Suga, S. Seki, J. Non-Cryst. Solids 16 (1974) 171.
[48] H. Suga, S. Seki, Faraday Discuss. 69 (1980) 221.
[49] H. Suga, Ann. N.Y. Acad. Sci. 484 (1986) 248.
[50] H. Suga, Thermochim. Acta 224 (1994) 69.
[51] W. Cahn, Nature 253 (1975) 310.
[52] H. Suga, S. Seki, in: W. Cahn (Ed.), Encyclopedia of Material Sciences and Engineering, Suppl. I, Pergamon Press, Oxford, 1988, p. 190.
[53] K. Adachi, H. Suga, S. Seki, Bull. Chem. Soc. Jpn. 41 (1968) 1073.
[54] K. Adachi, H. Suga, S. Seki, Bull. Chem. Soc. Jpn. 43 (1972) 1917.
[55] K. Adachi, H. Suga, S. Seki, Mol. Cryst. 18 (1972) 345.
[56] I. Kishimoto, J.-J. Pinvidic, T. Matsuo, H. Suga, Proc. Jpn. Acad. 67B (1991) 607.
[57] D. Eisenberg, W. Kauzmann, The Structure and Properties of Water, Clarendon Press, Oxford, 1969.
[58] O. Haida, T. Matsuo, H. Suga, S. Seki, J. Chem. Thermodyn. 6 (1974) 815.
[59] Y. Tajima, T. Matsuo, H. Suga, Nature 299 (1982) 810.
[60] H. Suga, T. Matsuo, Pure Appl. Chem. 64 (1992) 17.
[61] H. Suga, Thermochim. Acta 300 (1997) 117.
[62] M. Reiner, Phys. Today 17 (1964) 62.
[63] D.W. Davidson, in: F. Franks (Ed.), Water — A Comprehensive Treatise, Vol. 2, Plenum Press, New York, 1973, p. 115.
[64] O. Yamamuro, H. Suga, J. Thermal Anal. 35 (1989) 2025.
[65] H. Suga, T. Matsuo, O. Yamamuro, Supramol. Chem. 1 (1993) 221.
[66] S. Kawada, J. Phys. Soc. Jpn. 28 (1970) 265.
[67] S. Kawada, J. Phys. Soc. Jpn. 44 (1978) 1881.
[68] W. Gotze, L. Sjogren, Rep. Prog. Phys. 55 (1992) 241.
[69] O. Yamamuro, S. Takahara, A. Inaba, T. Matsuo, H. Suga, J. Phys. Condens. Matter 6 (1994) L169.
[70] O. Mishima, E. Stanley, Nature 396 (1998) 329.